Available online at www.sciencedirect.com
SCIENCE DIRECT®
ELSEVIER Applied Mathematics and Computation 175 (2006) 149–170
APPLIED MATHEMATICS AND COMPUTATION
www.elsevier.com/locate/amc

Analytical and numerical investigation of the Fredholm integral equation for the heat radiation problem

Naji Qatanani [a,*], Monika Schulz [b]

[a] *Department of Mathematics, College of Science and Technology, Al-Quds University, P.O. Box 20002, Abu Dies, Jerusalem, Israel*
[b] *University of Stuttgart, Mathematical Institute A, Pfaffenwaldring 57, D-70569 Stuttgart, Germany*

Abstract

This article deals with the mathematical and the numerical aspects of the Fredholm integral equation of the second kind arising as a result of the heat energy exchange inside a convex and non-convex enclosure geometries. Some mathematical results concerning the integral operator are presented. The Banach fixed point theorem is used to guarantee the existence and the uniqueness of the solution of the integral equation. For the non-convex geometries the visibility function has to be taken into consideration, then a geometrical algorithm is developed to provide an efficient detection of the shadow zones. For the numerical simulation of the integral equation we use the boundary element method based on the Galerkin discretization scheme. Some iterative methods for the discrete radiosity equation are implemented. Several two- and three-dimensional numerical test cases for convex and non-convex geometries are included. This give concrete hints which iterative scheme might be more useful for such practical applications.

* Corresponding author.
E-mail addresses: nqatanani@science.alquds.edu (N. Qatanani), moni@mathematik.uni-stuttgart.de (M. Schulz).

0096-3003/$ - see front matter
doi:10.1016/j.amc.2005.07.017

Keywords: Heat radiation; Fredholm integral equation; Boundary element method; Iterative methods; Galerkin scheme

1. Introduction

All bodies at temperature above absolute zero emit energy in a form of electromagnetic waves. A portion of this energy flux when impinging other bodies is absorbed. As a result, net energy flux occurs from a body of higher temperature to a body having lower temperature. This mode of energy transfer is known as heat radiation. The wavelength range encompassed by thermal radiation is approximately 0.1–100 μm. Heat radiation is, as each wave propagation phenomenon, of dual nature. It possesses the continuity properties of electromagnetic waves and the corpuscular properties characteristic for photons.

Heat radiation plays a dominant role in engineering and modern technology. One of the factors that accounts for the importance of the thermal radiation in some applications is the manner in which radiant emission depends on temperature. Another characteristic feature of radiation is that it can be transferred directly from one location to another only when the point can be seen when looking from another, i.e., it does not lay in the shadow zone. The presence of shadow zones should be taken into account in heat radiation calculation. This leads to a rather complex algorithm and long computing times.

It is evident that almost all phenomena that modelers deal with are governed by differential equations, however, heat radiation is one of the few phenomena governed by an integral equation. Due to this nice feature, the idea of using boundary element method for the solution of radiation problems naturally arises. Boundary element methods together with other numerical methods for different types of heat radiation problems have been addressed in [1–5,12–16,20].

In this present work we focus on the mathematical and the numerical aspects of the radiosity equation defined for convex and non-convex enclosure geometries with diffuse and grey surfaces. The organization of this paper is as follows:

In Section 2, we derive the heat radiosity equation for convex and non-convex geometries.

In Section 3, we present some important properties of the integral operator.

In Section 4, the Banach fixed point theorem is used to prove the existence and the uniqueness of the solution of the radiosity equation.

In Section 5, we discuss the numerical treatment of the integral equation. This leads us to the boundary element method based on the Galerkin discretization scheme. Moreover, it includes the realization of the visibility function.

In Section 6, we present four iterative methods, namely: the Picard iteration, the two- and multi-grid iterations and the conjugate gradient iteration for the discrete radiosity equation. Several 2D and 3D numerical test problems for the convex and the non-convex enclosure geometries are considered.

In Section 7, we give some concluding remarks about the numerical results related to the iterative methods.

2. The formulation of the problem

We consider an enclosure $\Omega \subset \mathbb{R}^d,\ d = 2, 3$ with a diffuse and grey surface Γ as shown in Fig. 1. We say that a surface is diffuse as emitter (reflector) if it emits (reflects) heat uniformly in every direction. For a grey surface the emissivity and reflectivity are independent of the wavelength (color) of the radiation. Thus, only the total intensity of radiation and not its spectrum is needed in a heat balance model. On Γ we assume, for simplicity, that the temperature is given.

Under the above assumptions the heat balance on Γ is given by

$$R - q_0 + J = 0, \tag{2.1}$$

where R is the heat brought to the surface by conduction, q_0 is the radiation emitted by the surface Γ, J is the energy of incoming irradiation on Γ.

For diffuse and grey surfaces the intensity of emitted radiation has the form

$$q_0 = \varepsilon\sigma T^4 + \varrho J. \tag{2.2}$$

The first part of Eq. (2.2) corresponds to the Stefan–Boltzmann radiation law, with ε is the emissivity coefficient $(0 < \varepsilon < 1)$, σ is the Stefan–Boltzmann

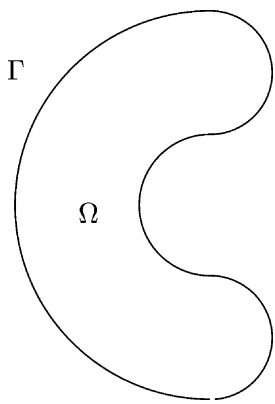

Fig. 1. Enclosure geometry.

constant which has the value $5.669996 \times 10^{-8}\ \frac{\mathrm{W}}{\mathrm{m}^2\,\mathrm{K}^4}$, ϱ is the reflection coefficient with the relation, $\varrho = 1 - \varepsilon$ for opaque grey surfaces.

Eq. (2.2) with $\varrho = 1 - \varepsilon$ can be rewritten as

$$q_0 = \varepsilon\sigma T^4 + (1-\varepsilon)J. \tag{2.3}$$

In the case of non-convex geometries, the irradiation on Γ depends only on the radiation emitted by different parts of Γ itself. Consequently, we can write for any point $x \in \Gamma$

$$J(x) = \int_\Gamma W^*(x,y) q_0(y) V(x,y)\,\mathrm{d}\Gamma_y, \tag{2.4}$$

where $W^*(x,y)$ is called the view factor between the points x and y of Γ. For general enclosure geometries $W^*(x,y)$ has the representation [12,20]

$$W^*(x,y) = \frac{\cos\theta_x \cdot \cos\theta_y}{c_0|x-y|^{d-1}} \tag{2.5}$$

or equivalently

$$W^*(x,y) = \frac{[n_y \cdot (y-x)] \cdot [n_x \cdot (x-y)]}{c_0|x-y|^{d+1}}, \tag{2.6}$$

where $c_0 = 2$ for $d = 2$ and $c_0 = \pi$ for $d = 3$.

In this, n_x is the inner normal to Γ at the point x and θ_x denotes the angle between n_x and $x - y$, n_y and θ_y are defined analogously. The function $V(x,y)$ in (2.4) is called the visibility function. More precisely, if the points x and y can "see each other" along a straight line segment that does not intersect Γ at any other point, then $V(x,y) = 1$; otherwise $V(x,y) = 0$.

Substituting Eq. (2.4) into Eq. (2.3) we obtain for any point $x \in \Gamma$

$$q_0(x) = \varepsilon(x)\sigma T^4(x) + (1-\varepsilon(x)) \int_\Gamma W(x,y) q_0(y)\,\mathrm{d}\Gamma_y \quad \text{for } x \in \Gamma, \tag{2.7}$$

where the kernel $W(x,y)$ is given by

$$W(x,y) = W^*(x,y)V(x,y). \tag{2.8}$$

Since $V(x,y)$ and $W^*(x,y)$ are symmetric functions, it follows that $W(x,y)$ is also symmetric.

3. Properties of the integral operator

Eq. (2.7) is a Fredholm boundary integral equation of the second kind. We introduce the integral operator $\widetilde{K} : L^\infty(\Gamma) \to L^\infty(\Gamma)$ with

$$\widetilde{K} q_0(x) := \int_\Gamma W(x,y) q_0(y)\,\mathrm{d}\Gamma_y \quad \text{for } x \in \Gamma,\ \ q_0 \in L^\infty(\Gamma). \tag{3.1}$$

This integral operator has the following properties:

Lemma 1. *Let Γ be a Ljapunow surface in $C^{1,\delta}$ with $\delta \in [0,1)$. Then for any arbitrary point $x \in \Gamma$ we obtain*

$$\int_{\Gamma} W^*(x,y)\,\mathrm{d}\Gamma_y = 1,$$

where $W^*(x,y)$ is given by (2.6).

Proof. First we choose a local coordinate system in the point $x \in \Gamma$ so that $x = (0,0,0)$ and the plane (ξ_1,ξ_2) is tangent to Γ in x. Furthermore, we choose $y = (\xi_1,\xi_2,f(\xi_1,\xi_2))$ in the neighbourhood of $\xi_1 = \xi_2 = 0$. Using the assumption that $\Gamma \in C^{1,\delta}$ with $\delta \in [0,1)$ together with the Taylor expansion of y in the local coordinate system and some trivial estimates (see [12]) we get the following inequalities:

$$\left|\frac{n(x)\cdot(y-x)}{|y-x|^2}\right| \leqslant c_1|\xi_\alpha|^{\delta-1} \quad \text{and} \quad \left|\frac{n(y)\cdot(x-y)}{|x-y|^2}\right| \leqslant c_2|\xi_\alpha|^{\delta-1} \tag{3.2}$$

with $\alpha \in [1,d-1]$ and $d = 2$ or 3. Consequently, one obtains form (3.2)

$$|W^*(x,y)| \leqslant c_3|\xi_\alpha|^{-2(1-\delta)+3-d} \tag{3.3}$$

with an arbitrary constant c_3 and $d = 2$ or 3. This shows that $W^*(x,y)$ is a weakly singular kernel of type $|x-y|^{-2(1-\delta)}$ and hence it is integrable.

In order to calculate $\int_\Gamma W^*(x,y)\,\mathrm{d}\Gamma_y$ we use Stoke's theorem [12,20–22]. For the following we consider a closed surface Γ and an arbitrary point $y = (y_1,y_2,y_3) \in \Gamma$. At this point the normal to the area A is constructed. Let the functions $P_1(y)$, $P_2(y)$ and $P_3(y)$ be any twice-differentiable functions of y_1, y_2 and y_3 and n is the normal. Stoke's theorem in three dimensions provides the following relation:

$$\begin{aligned}&\int_{\partial A}(P_1\,\mathrm{d}y_1 + P_2\,\mathrm{d}y_2 + P_3\,\mathrm{d}y_3)\\ &\quad = \int_A\left[\left(\frac{\partial P_3}{\partial y_2} - \frac{\partial P_2}{\partial y_3}\right)n_1(y) + \left(\frac{\partial P_1}{\partial y_3} - \frac{\partial P_3}{\partial y_1}\right)n_2(y) + \left(\frac{\partial p_2}{\partial y_1} - \frac{\partial P_1}{\partial y_2}\right)n_3(y)\right]\mathrm{d}A.\end{aligned} \tag{3.4}$$

Hence this relation can now be applied to express area integrals in view factor computations in terms of boundary integrals. To this end, we consider the surface Γ as shown in Fig. 2 and let $\Gamma_\gamma = Z(x,\gamma) \cap \Gamma$ be a small neighbourhood of the point x and define $\Gamma^* = \Gamma \backslash \Gamma_\gamma$.

Here $Z(x,\gamma)$ is a cylinder which is defined by the relation $x_1^2 + x_2^2 = \gamma^2$. Since Γ^* is not independent of x the integral $\int_\Gamma W^*(x,y)\,\mathrm{d}\Gamma_y$ can be expressed as

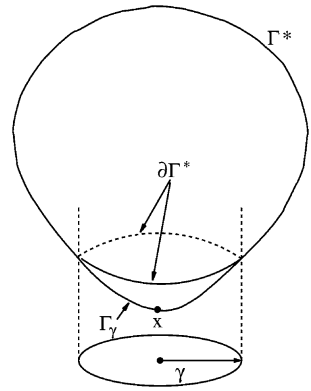

Fig. 2. Convex case.

$$F(x) = \int_{\Gamma} W^*(x,y)\,\mathrm{d}\Gamma_y = \int_{\Gamma_\gamma} W^*(x,y)\,\mathrm{d}\Gamma_y + \int_{\gamma^*} W^*(x,y)\,\mathrm{d}\Gamma_y, \tag{3.5}$$

where the first integral tends to zero for $\gamma \to 0$ because of the weakly singular kernel $W^*(x,y)$. Hence (3.5) is reduced to

$$F_\gamma(x) = \lim_{\gamma\to 0} \int_{\Gamma^*} W^*(x,y)\,\mathrm{d}\Gamma_y. \tag{3.6}$$

Since the view factor $W^*(x,y)$ is smooth in Γ^* the application of Stoke's theorem leads to

$$\begin{aligned} F_\gamma(x) &= \lim_{\gamma\to 0} \int_{\Gamma^*} W^*(x,y)\,\mathrm{d}\Gamma_y = \lim_{\gamma\to 0} \int_{\partial\Gamma^*} \nabla \times \vec{P}(y)\cdot n(y)\,\mathrm{d}y \\ &= \lim_{\gamma\to 0} \oint_{\partial\gamma^*} (P_1\,\mathrm{d}y_1 + P_2\,\mathrm{d}y_2 + P_3\,\mathrm{d}y_3), \end{aligned} \tag{3.7}$$

where $P_1(y)$, $P_2(y)$ and $P_3(y)$ are given respectively by

$$\begin{aligned} P_1(y) &= \frac{-n_2(x)(x_3-y_3) + n_3(x)(x_2-y_2)}{2\pi|x-y|^2}, \\ P_2(y) &= \frac{n_1(x)(x_3-y_3) - n_3(x)(x_1-y_1)}{2\pi|x-y|^2}, \\ P_3(y) &= \frac{-n_1(x)(x_2-y_2) + n_2(x)(x_1-y_1)}{2\pi|x-y|^2}. \end{aligned} \tag{3.8}$$

The normal to the area element is perpendicular to both the x_1- and x_2-axes and parallel to the x_3-axis. Hence (3.7) becomes

$$F_\gamma(x) = \frac{1}{2\pi}\lim_{\gamma\to 0}\oint_{\partial\Gamma^*}\frac{(x_2-y_2)\,\mathrm{d}y_1-(x_1-y_1)\,\mathrm{d}y_2}{|x-y|^2}$$
$$= \frac{1}{2\pi}\lim_{\gamma\to 0}\oint_{\partial\Gamma^*}\frac{-y_2\,\mathrm{d}y_1+y_1\,\mathrm{d}y_2}{y_1^2+y_2^2+y_3^2} \tag{3.9}$$

using the fact that the area element is located at the origin of the coordinate system. With the help of the relation $y_1^2+y_2^2=\gamma^2$ we get

$$F_\gamma(x) = \underbrace{\frac{1}{2\pi}\lim_{\gamma\to 0}\oint_{\partial\Gamma^*}\frac{1}{\gamma^2}(-y_2\,\mathrm{d}y_1+y_1\,\mathrm{d}y_2)}_{:=I_1} + \underbrace{\frac{1}{2\pi}\lim_{\gamma\to 0}\oint_{\partial\Gamma^*}\frac{-y_3^2(-y_2\,\mathrm{d}y_1+y_1\,\mathrm{d}y_2)}{(\gamma^2+y_3^2)\gamma^2}}_{:=I_2}. \tag{3.10}$$

Let the boundary of the domain Γ^* be described by the triple $(y_1,y_2,f(y,y_2))$ then the first integral I_1 will be integrated over the circle $y_1^2+y_2^2=\gamma^2$. Using the polar coordinates $y_1=\gamma\cos\theta$ and $y_2=\gamma\sin\theta$ one obtains directly

$$I_1 = \frac{1}{2\pi}\cdot\frac{1}{\gamma^2}\int_0^{2\pi}\gamma^2\,\mathrm{d}\theta = 1.$$

For the second integral we have $y_3=f(y_1,y_2)$. Applying Taylor's expansion it can easily be shown that $I_2=0$. Hence, we have the desired result for convex enclosure geometries

$$\int_\Gamma W^*(x,y)\,\mathrm{d}\Gamma_y = 1.$$

Next we have to show that this result holds also for the non-convex case, see Fig. 3. Therefore we consider the set $\Gamma\backslash\Gamma_y$, where $\Gamma_y=\{x\in\Gamma\,|\,V(x,y)=1\}$.

This set consists in general of many disjoint components. For the sake of simplicity, we take one of these components and denote it by D_i. Due to the discontinuity of the visibility function $V(x,y)$, the Stoke's theorem cannot be applied directly for $W(x,y)$, but we write first

$$\int_{\Gamma^*} W(x,y)\,\mathrm{d}\Gamma_y = \int_{\Gamma^*} W^*(x,y)\,\mathrm{d}\Gamma_y - \sum_i\int_{D_i}\nabla\times P_x(y)\cdot n(y)\,\mathrm{d}y.$$

Since the second integral vanishes over the closed surface D_i, the assertion follows directly. □

Lemma 2. *Let Γ be a closed surface of the class C^2. Then $W^*(x,y)$ in (2.6) is a bounded kernel, i.e.,*

$$|W^*(x,y)|\leqslant\widetilde{C}$$

with a suitable chosen constant $\widetilde{C}$.

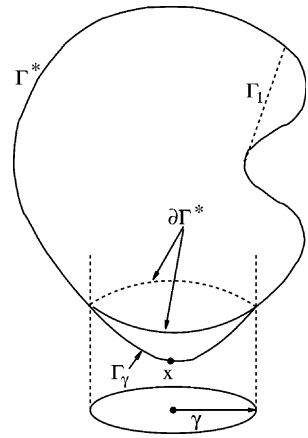

Fig. 3. Non-convex case.

Proof. Under the assumption that $\Gamma \subset C^2$ the following requirements are fulfilled:

1. In every point of the surface exists a tangential plane.
2. If θ is the angle between the normals at the points x and y, and $r_{1,2}$ denotes the distance between these two points the inequality
$$|\theta| < Ar_{1,2}, \quad \theta \in (0, 2\pi) \tag{3.11}$$
holds, where A is a positive number independent from the choice of the points x and y.
3. For all points x_0 of the surface there exists a fixed number d with the property that the point of the surface which is located within the sphere of radius d around x_0, is intersected by a parallel to the normal in x_0 at most in one point.

Let the ζ-axis be the normal at the surface point x_0 and take the two ξ- and η-axes to be the tangential plane containing the point x_0 such that the three axes form an orthonormal system. The corresponding unit vectors are denoted by e_1, e_2 and e_3. As a consequence of the third condition above a part of the surface which lies inside the Ljapunow sphere takes the form $\zeta = \Psi(\xi, \eta)$. The existence of the tangential plane and its continuous change imply the existence of the first partial derivatives Ψ_ξ and Ψ_η which are continuous due to requirement 2. Assuming that d is sufficiently small, i.e.,
$$Ad \leqslant 1, \tag{3.12}$$
so that the angle between the normal at x_0 and the normal at any arbitrary point of the surface which lies inside the sphere does not exceed the value $\frac{\pi}{2}$. Denoting with r_0 the distance $|x_0 - y_0|$, so one obtains

$$\cos\theta_0 \geqslant 1-\frac{1}{2}\theta_0^2 \geqslant 1-\frac{1}{2}A^2r_0^2 > \frac{1}{2}. \tag{3.13}$$

On the other hand we have

$$\frac{1}{\cos\theta_0} = \sqrt{1+\Psi_\xi^2+\Psi_\eta^2} \leqslant 1+A^2r_0^2 \leqslant 2 \tag{3.14}$$

and therefore

$$\Psi_\xi^2+\Psi_\eta^2 \leqslant 2A^2r_0^2+A^4r_0^2. \tag{3.15}$$

The introduction of the polar coordinates $\xi=\varrho_0\cos\theta$, $\eta=\varrho_0\sin\theta$ leads to

$$\Psi_{\varrho 0}^2 = (\Psi_\xi\cos\theta+\Psi_\eta\sin\theta)^2 \leqslant \Psi_\xi^2+\Psi_\eta^2.$$

Using (3.15) together with the estimate $|\Psi|\leqslant\sqrt{3}\varrho_0$ and therefore $r_0\leqslant 2\varrho_0$ we get

$$|\Psi_{\varrho_0}| \leqslant 2\sqrt{3}A_{\varrho_0}. \tag{3.16}$$

Finally, it follows from (3.13) that

$$1-\cos\theta_0 \leqslant 2A^2\varrho_0^2. \tag{3.17}$$

As a consequence of (3.15) the estimate

$$|\cos(n,e_1)| = \frac{\sqrt{\Psi_\xi^2+\Psi_\eta^2}}{\sqrt{1+\Psi_\xi^2+\Psi_\eta^2}} \leqslant |\Psi_\xi| \leqslant \sqrt{3}Ar_0 \tag{3.18}$$

holds, where n is the unit vector of the outward normal of Γ at an arbitrary point. Analogously we get

$$|\cos(n,e_2)| \leqslant \sqrt{3}Ar_0 \quad \text{and} \quad |\cos(n,e_3)| = \cos\theta_0. \tag{3.19}$$

Summarizing the estimates above, we get

$$|\Psi| \leqslant c\varrho_0^2, \quad |\cos(n,e_1)| < c\varrho_0, \quad |\cos(n,e_2)| \leqslant c\varrho_0, \quad |\cos(n,e_3)| \geqslant \frac{1}{2}. \tag{3.20}$$

From (3.18) it follows:

$$|\cos((x-y),n(x))| = \left|\frac{n(x)\cdot(x-y)}{r_{1,2}}\right| \leqslant \Psi_\xi \leqslant D_1r_{1,2} \tag{3.21}$$

and similarly the estimate

$$|\cos((y-x),n(y))| = \left|\frac{n(y)\cdot(y-x)}{r_{1,2}}\right| \leqslant D_1r_{1,2} \tag{3.22}$$

with $D_1 = \sqrt{3}A$. Therefore we get for the kernel

$$|W^*(x,y)| = \left|\frac{\cos((x-y),n(x))\cdot\cos((y-x),n(y))}{r_{1,2}^2}\right| \leqslant \tilde{c}, \tag{3.23}$$

where $\tilde{c} = \frac{3A^2}{\pi}$ with $A = \sup_{x,y\in\Gamma}\left(\frac{\theta}{r_{1,2}}\right)$. □

Let us remark that in the two-dimensional case for $G^*(x,y)$ in (2.6) the estimate

$$|W^*(x,y)| \leqslant \tilde{c} r_{1,2}$$

holds with some constant $\tilde{c}$.

Lemma 3. *For the integral kernel $W(x,y)$ it holds $W(x,y) \geqslant 0$. The mapping $\widetilde{K} : L^p(\Gamma) \to L^p(\Gamma)$ is compact for $1 \leqslant p \leqslant \infty$. Furthermore, we get*

(a) $\|\widetilde{K}\| = 1$ *in* L^p *for* $1 \leqslant p \leqslant \infty$.
(b) *The spectral radius* $\varrho(\widetilde{K}) = 1$.

Proof. For the convex case, $W^*(x,y)$ is obviously not negative. For the non-convex case the visibility factor $V(x,y) \equiv 0$ whenever $W^*(x,y) < 0$, hence $W(x,y) \geqslant 0$ and, consequently, the integral operator $\widetilde{K}$ is not negative.

From Lemma 1 follows that the kernel $W(x,y)$ is integrable and $\widetilde{K}$ is a weakly singular integral operator. Hence, the mapping $\widetilde{K} : L^p(\Gamma) \to L^p(\Gamma)$ is compact. We now estimate the norm of this integral operator $\widetilde{K}$. For $1 < p < \infty$ and $q_0 \in L^p(\Gamma)$ we have with $\frac{1}{p} + \frac{1}{q} = 1$

$$\begin{aligned}|\widetilde{K}q_0(x)| &= \left|\int_{\Gamma_y} W(x,y)^{\frac{1}{p}+\frac{1}{q}} q_0(y)\,\mathrm{d}\Gamma_y\right| \\ &\leqslant \left(\int_{\Gamma_y} W(x,y)\,\mathrm{d}\Gamma_y\right)^{\frac{1}{q}}\left(\int_{\Gamma_y} W(x,y)|q_0(y)|^p\,\mathrm{d}\Gamma_y\right)^{\frac{1}{p}}.\end{aligned} \tag{3.24}$$

Since $\int_{\Gamma_y} W(x,y)\,\mathrm{d}\Gamma_y = 1$ (see Lemma 1) it follows:

$$|\widetilde{K}q_0(x)| \leqslant \left(\int_{\Gamma_y} W(x,y)|q_0(y)|^p\,\mathrm{d}\Gamma_y\right)^{\frac{1}{p}}. \tag{3.25}$$

Furthermore we get

$$\begin{aligned}\|\widetilde{K}q_0(x)\|_{L^p}^p &= \int_{\Gamma_x} |\widetilde{K}q_0(x)|^p\,\mathrm{d}\Gamma_x \leqslant \int_{\Gamma_y} |q_0(y)|^p \\ &\quad\times \int_{\Gamma_x} W(x,y)\,\mathrm{d}\Gamma_x\,\mathrm{d}\Gamma_y = \|q_0(y)\|_{L^p}^p.\end{aligned} \tag{3.26}$$

Hence we obtain $\|\widetilde{K}\| \leqslant 1$ in all spaces L^p, $1 \leqslant p \leqslant \infty$. Equality can be achieved by choosing $q_0 = 1$ which is clearly an eigenvector of $\widetilde{K}$ with eigenvalue 1.

Finally it follows from the fact $\widetilde{K}1 = 1$ and the Hilbert theorem that the integral operator $\widetilde{K}$ has an eigenvalue λ_0 with $|\lambda_0| = \|\widetilde{K}\| = 1$. □

Lemma 4. *The integral operator $\widetilde{K}$ is for the convex case, i.e., $V(x,y) \equiv 1$, a classical pseudodifferential operator of order $\alpha = -2$. The kernel of this integral operator possesses a pseudohomogeneous expansion of the form*

$$W^*(x,y) \sim |u-v|^{-\alpha-2} \sum_{v \geqslant 0} \Psi_v(x,\theta)|u-v|^v \sim r^{-\alpha-2} \sum_{v \geqslant 0} \Psi_v(x,\theta) r^v. \tag{3.27}$$

In the two-dimensional (either convex or non-convex) case, the kernel possesses a pseudohomogeneous expansion of the form

$$W^*(x,y) \sim (s-s_0) \sum_{v \geqslant 0} C_v(x)(s-s_0)^v. \tag{3.28}$$

In the two-dimensional convex case the integral operator $\widetilde{K}$ is even a pseudodifferential operator of order $-\infty$.

Proof. One can write the kernel of the integral operator $\widetilde{K}$ as a convolution kernel in a pseudohomogeneous expansion form. In the case when Γ has a quadratic parameter representation and $u = \Phi^{-1}(x)$ one obtains [19]

$$y - x = \Phi(v) = bv_1 + cv_2 + dv_1^2 + 2ev_1v_2 + fv_2^2$$

with vectors $b, c, d, e, f \in \mathbb{R}^3$. For the normal, one has

$$n(v) = \frac{\Phi_1 \times \Phi_2}{|\Phi_1 \times \Phi_2|},$$

where Φ_1 and Φ_2 are given by the parameter representation of Γ as

$$\Phi_1 = \frac{\partial \Phi}{\partial v_1} = b + 2(v_1 d + v_2 e), \qquad \Phi_2 = \frac{\partial \Phi}{\partial v_2} = e + 2(v_1 e + v_2 f)$$

and

$$\Phi_1 \times \Phi_2 = b \times c + 2Q_1(v) + 4Q_2(v)$$

with

$$Q_1(v) = v_1(b \times e + d \times c) + v_2(b \times f + e \times c),$$
$$Q_2(v) = v_1^2(d \times e) + v_1 v_2(d \times f) + v_2^2(e \times f).$$

Consequently

$$(\Phi_1 \times \Phi_2)(y-x) = v_1^2 b(d \times c) + 2v_1 v_2 c(b \times e) + v_2^2 c(b \times f).$$

Using the polar coordinates in the parameter plane $v - u = r(\cos\theta, \sin\theta)^{\mathrm{T}}$ we obtain

$$n(y)\cdot(y-x) = \frac{r^2}{|\Phi_1 \times \Phi_2|}[b(d\times c)\cos^2\theta + 2c(b\times e)\cos\theta\sin\theta + c(b\times f)\sin^2\theta]. \tag{3.29}$$

Analogously $n(x)(x-y)$ has in $u = \Phi^{-1}(x) = 0$ an expansion of the form

$$n(x)\cdot(x-y) = \frac{-(b\times c)}{|b\times c|} r^2[d\cos^2\theta + 2e\cos\theta\sin\theta + f\sin^2\theta]. \tag{3.30}$$

From [19] it holds also

$$\varrho^{-4} = |x-y|^{-4} = r^{-4}\sum_{v=0}^{\infty}(\ell_2^{-2-v}(\theta)P_{3v}(\cos\theta,\sin\theta))r^v,$$

where P_{3v} is a homogeneous polynomial of degree $3v$ and $\ell_2(\theta)$ is given by

$$\ell_2(\theta) = |b|^2\cos^2\theta + bc\sin\theta\cos\theta + |c|^2\sin^2\theta.$$

Finally, one obtains for $W^*(x,y)$ in (2.6) the expansion

$$W^*(x,y) = \frac{|b\times c|}{4\pi|\Phi_1\times\Phi_2|}\left\{[L\cos^2\theta + 2M\cos\theta\sin\theta + N\sin^2\theta]^2 \times\sum_{v=0}^{\infty}(\ell_2^{-2-v}P_{3v})(\theta)r^v\right\}, \tag{3.31}$$

where L, M and N are the coefficients of the second fundamental form defined by

$$d(b\times c) = -(d\times c)b = -\frac{1}{2}|b\times c|L,$$
$$e(b\times c) = -(b\times e)c = -\frac{1}{2}|b\times c|M,$$
$$f(b\times c) = -(d\times f)c = -\frac{1}{2}|b\times c|N.$$

From (3.31) follows that the integral operator $\widetilde{K}$ is for $V(x,y)\equiv 1$, i.e., for convex Γ a classical pseudodifferential operator of the order $\alpha = -2$. The kernel possesses a pseudohomogeneous expansion of the form

$$W^*(x,y) \sim |u-v|^{-\alpha-2}\sum_{v\geqslant 0}\Phi_v(x,\theta)|u-v|^v$$
$$\sim r^{-\alpha-2}\sum_{v\geqslant 0}\Phi_v(x,\theta)r^v. \qquad \square \tag{3.32}$$

Lemma 5. *Let Γ be any closed curve of the class C^2. Then in the two-dimensional case $\widetilde{K}$ defines a continuous mapping $\widetilde{K} : L^2(\Gamma) \to H^1(\Gamma)$ if $W(x,y)$ is the kernel of the radiosity equation as defined in (2.6) and (2.8).*

Proof. First let $W^*(x,y)$ be defined as in (2.6) and

$$\Phi(x) = \int_\Gamma W^*(x,y)V(x,y)q_0(y)\,\mathrm{d}\Gamma_y. \tag{3.33}$$

Consider the simple case similar to the situation in Fig. 4.

We use the following abbreviations $y = y(s)$, $x^{(i)} = x(\sigma^{(i)})$ with $\sigma^{(i)} = \sigma^{(i)}(\sigma)$ for $i = 1,2$. Γ^+ and Γ^- are open parts with $x(\sigma_1^*), x(\sigma_2^*) \notin \Gamma^+$, Γ^- and $x(\sigma_1^*), x(\sigma_2^*) \in \overline{\Gamma}^+, \overline{\Gamma}^-$.

Choose $\sigma^{(1)}$ in such a way that $x(\sigma_1^*) - x(\sigma)$ is for all $\sigma_1^* \in (\sigma, \sigma^{(1)})$ no longer parallel to $x^{(2)} - x(\sigma)$. Then with the help of these abbreviations, Eq. (3.33) can be expressed as

$$\Phi(x(\sigma)) = \int_{x(\sigma^{(2)})}^{x(\sigma^{(1)})} W^*(x(\sigma), y(s))q_0(y(s))\,\mathrm{d}\Gamma_{y(s)}. \tag{3.34}$$

Applying Leibniz rule of differentiation, one obtains

$$\begin{aligned}\frac{\mathrm{d}\Phi(\sigma)}{\mathrm{d}\sigma} = &\int_{x(\sigma^{(2)})}^{x(\sigma^{(1)})} \frac{\mathrm{d}W^*(x(\sigma), y(s))}{\mathrm{d}\sigma} \cdot q_0(y(s))\,\mathrm{d}\Gamma_{y(s)} \\ &+ \frac{\mathrm{d}x(\sigma^{(1)})}{\mathrm{d}\sigma} \cdot W^*(x(\sigma), x(\sigma^{(1)})) \cdot q_0(x(\sigma^{(1)})) \\ &- \frac{\mathrm{d}x(\sigma^{(2)})}{\mathrm{d}\sigma} \cdot W^*(x(\sigma), x(\sigma^{(2)})) \cdot q_0(x(\sigma^{(2)})).\end{aligned} \tag{3.35}$$

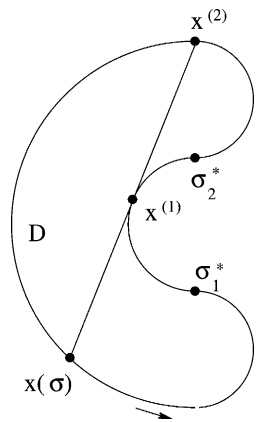

Fig. 4. Parametric representation.

Since the normal at the point $x^{(1)}$ is perpendicular to the straight line between $x(\sigma)$ and $x^{(2)}$ the kernel $W^*(x(\sigma), x(\sigma^{(1)})) = 0$ and therefore Eq. (3.35) is reduced to

$$\frac{\mathrm{d}\Phi(\sigma)}{\mathrm{d}\sigma} = \int_{x(\sigma^{(2)})}^{x(\sigma^{(1)})} \frac{\mathrm{d}W^*(x(\sigma), y(s))}{\mathrm{d}\sigma} \cdot q_0(y(s))\,\mathrm{d}\Gamma_{y(s)} - \frac{\mathrm{d}x(\sigma^{(2)})}{\mathrm{d}\sigma} \cdot W^*(x(\sigma), x(\sigma^{(2)})) \cdot q_0(x(\sigma^{(2)})). \tag{3.36}$$

For $\Gamma \in C^2$ follows that $W^*(x(\sigma), y(s))$ and $\frac{\mathrm{d}W^*}{\mathrm{d}\sigma}(x(\sigma), y(s))$ are continuous kernels and therefore the integral

$$I = \int_{x(\sigma^{(2)})}^{x(\sigma^{(1)})} \frac{\mathrm{d}W^*(x(\sigma), y(s))}{\mathrm{d}\sigma} \cdot q_0(y(s))\,\mathrm{d}\Gamma_{y(s)} \quad \text{for } q_0(y(s)) \in L^2(\Gamma)$$

is bounded in $L^2(\Gamma)$. From the definition of $x^{(2)}$ we obtain

$$\frac{\mathrm{d}\sigma^{(2)} \cdot \cos((x^{(2)} - x), n(\sigma^{(2)}))}{(|x^{(2)} - x(\sigma)| - |x^{(1)} - x(\sigma)|)} = \frac{\mathrm{d}\sigma \cdot \cos((x - x^{(2)}), n(\sigma))}{|x^{(1)} - x(\sigma)|} \tag{3.37}$$

and since $(x - x^{(2)})$ and $(x - x^{(1)})$ are parallel this leads to

$$\frac{\mathrm{d}\sigma^{(2)}}{\mathrm{d}\sigma} W^*(x(\sigma), x(\sigma^{(2)})) = \frac{(|x^{(2)} - x(\sigma)| - |x^{(1)} - x(\sigma)|)}{|x^{(1)} - x(\sigma)||x^{(2)} - x|} \cdot \cos^2((x - x^{(1)}), n(\sigma)). \tag{3.38}$$

A continuous curve with non-vanishing curvature is also a C-curve [6], i.e., there exists constants $c_0 > 0$, $c_1 > 0$ such that for all points on the curve we have

$$|x(\sigma^{(1)}) - x(\sigma)| \leqslant |\sigma^{(1)} - \sigma| \leqslant c_0 |x^{(1)} - x(\sigma)| \quad \text{and}$$
$$|\cos((x - x^{(1)}), n(\sigma))| \leqslant c_1 |\sigma^{(1)} - \sigma|.$$

All together we obtain the estimate

$$\left| \frac{\mathrm{d}\sigma^{(2)}}{\mathrm{d}\sigma} W^*(x(\sigma), x^{(2)}) \right| \leqslant 1 \cdot c_0 \cdot c_1^2 |\sigma^{(1)} - \sigma| \leqslant M_1 \tag{3.39}$$

and from Lemma 2 with a constant M_0 we know $|W^*(x(\sigma), x^{(2)})| \leqslant M_0$. This leads immediately to the following estimate:

$$\begin{aligned} &\left\| \frac{\mathrm{d}x(\sigma^{(2)})}{\mathrm{d}\sigma} \cdot W^*(x(\sigma), x(\sigma^{(2)})) \cdot q_0(x(\sigma^{(2)})) \right\|^2_{L^2(\Gamma)} \\ &= \int_\Gamma \left| \frac{\mathrm{d}\sigma^{(2)}}{\mathrm{d}\sigma} \cdot W^*(x(\sigma, x(\sigma^{(2)})) q_0(x(\sigma^{(2)})) \right|^2 \mathrm{d}\sigma \\ &\leqslant M_1 \cdot M_0 \int_\Gamma |q_0(\sigma^{(2)})|^2 \left| \frac{\mathrm{d}\sigma^{(2)}}{\mathrm{d}\sigma} \right| \mathrm{d}\sigma \leqslant M_1 \cdot M_0 \|q_0\|^2_{L^2(\Gamma)}, \end{aligned}$$

which shows the assertion. □

Lemma 6. *The integral operator $A = (I - K)$ is L^2-elliptic. Furthermore A is a positive definite operator which satisfies the Gårding inequality on Γ.*

Proof. Let the integral operator K be defined as $K = (I - \varepsilon)\widetilde{K}$, where $\widetilde{K}$ is given by (3.1). From Lemma 3 it follows that

$$\|Kq_0\|_{L^2(\Gamma)} \leqslant (1 - \varepsilon)\|q_o\|_{L^2(\Gamma)}. \tag{3.40}$$

Furthermore, K satisfies the inequality

$$\langle Kq_0, q_0\rangle_{L^2(\Gamma)} \leqslant (1 - \varepsilon)\langle q_0, q_0\rangle_{L^2(\Gamma)}. \tag{3.41}$$

Eq. (3.41) with $A = (I - K)$ leads to

$$\varepsilon\langle q_0, q_0\rangle_{L^2(\Gamma)} \leqslant \langle Aq_0, q_0\rangle_{L^2(\Gamma)} \leqslant (2 - \varepsilon)\langle q_0, q_0\rangle_{L^2(\Gamma)}. \tag{3.42}$$

Furthermore, A satisfies the Gårding inequality, i.e., for all $q_o \in L^2(\Gamma)$ and $\varepsilon \geqslant 0$ the following holds:

$$\mathrm{Re}(Aq_0, q_0) = \mathrm{Re}\int_\Gamma q_0 A q_0 \,\mathrm{d}\Gamma_x \geqslant \varepsilon\|q_0\|^2_{L^2(\Gamma)}. \qquad \square \tag{3.43}$$

4. Existence theorem for the radiosity integral equation

A simple method to prove the existence of the solution of the integral Eq. (2.7) is the application of Banach's fixed point theorem. The successive approximation method can be used and the convergence of the Neumann series can be proved. We want to show first, that the integral operator

$$K = (1 - \varepsilon)\widetilde{K} : L^p(\Gamma) \to L^p(\Gamma) \quad \text{for } 1 < p < \infty$$

defines a contraction mapping, i.e., there exists a constant $0 \leqslant c < 1$ such that

$$\|Kq_0 - K\widetilde{q_0}\|_{L^p(\Gamma)} \leqslant c\|q_0 - \widetilde{q_0}\|_{L^p(\Gamma)} \tag{4.1}$$

holds. From the definition

$$Kq_0 - K\widetilde{q_0} = (1 - \varepsilon)\int_\Gamma W(x, y)\cdot(q_0(y) - \widetilde{q_0}(y))\,\mathrm{d}\Gamma_y$$

and the application of Hölder's inequality follows:

$$|Kq_0 - K\widetilde{q_0}| \leqslant |(1 - \varepsilon)|\left(\int_\Gamma W(x, y)\,\mathrm{d}\Gamma_y\right)^{\frac{1}{q}} \cdot \left(\int_\Gamma W(x, y)|q_0 - \widetilde{q_0}|^p \,\mathrm{d}\Gamma_y\right)^{\frac{1}{p}} \tag{4.2}$$

with $\frac{1}{p}+\frac{1}{p}=1$. Since $\int_\Gamma W(x,y)\,d\Gamma_y = 1$ (see Lemma 1) we get

$$|Kq_0 - K\widetilde{q}_0| \leqslant |(1-\varepsilon)|\left(\int_\Gamma W(x,y)|q_0(y)-\widetilde{q}_0(y)|^p\,d\Gamma_y\right)^{\frac{1}{p}}. \tag{4.3}$$

Then one obtains

$$\|Kq_o - K\widetilde{q}_0\|^p_{L^p(\Gamma)} \leqslant |1-\varepsilon|^p \cdot \int_{\Gamma y}|q_0(y)-\widetilde{q}_0(y)|^p \int_{\Gamma_x} W(x,y)\,d\Gamma_x\,d\Gamma_y,$$

so that we finally have

$$\|Kq_o - K\widetilde{q}_0\|^p_{L^p(\Gamma)} \leqslant |(1-\varepsilon)|^p \cdot \|q_0(y)-\widetilde{q}_0(y)\|_{L^p(\Gamma)}.$$

Due to the inequality $0<\varepsilon<1$, for the constant c we get $c := |1-\varepsilon|^p < 1$. Hence the integral operator K is contractive on $L^p(\Gamma)$ and the iteration scheme $q_{0,n+1} = Kq_{0,n}$ for $n = 1,2,\ldots$ is convergent. $\{q_{0,n}\}$ converges to some q_0 in the space $L^p(\Gamma)$, which solves the equation $Kq_0 = q_0$ in $L^p(\Gamma)$. The uniqueness of $q_0 \in L^p(\Gamma)$ follows directly from the contraction of K due to

$$0 < \|q_0-\widetilde{q}_0\|_{L^p(\Gamma)} = \|Kq_0 - K\widetilde{q}_0\|_{L^p(\Gamma)} \leqslant c\cdot\|q_0-\widetilde{q}_0\|_{L^p(\Gamma)}, \quad c<1. \tag{4.4}$$

Consequently we have

$$(1-c)\cdot\|q_0-\widetilde{q}_0\|_{L^p(\Gamma)} \leqslant 0. \tag{4.5}$$

Since q_0 and $\widetilde{q}_0$ are two fixed points of K with $(1-c)>0$ and $\|q_0-\widetilde{q}_0\|>0$, then Eq. (4.5) implies $q_0 = \widetilde{q}_0$ and one gains the assertion.

5. The numerical treatment of the radiosity integral equation

5.1. Boundary element method

For the numerical simulation of the radiosity equation we use the boundary element method. The weak formulation of (2.7) in $L^2(\Gamma)$ reads: find $q_0 \in L^2(\Gamma)$ such that for all $u \in L^2(\Gamma)$ there holds

$$\int_\Gamma q_0(x)u(x)\,d\Gamma_x = \sigma\int_\Gamma \varepsilon T^4(x)u(x)\,d\Gamma_x + \int_\Gamma(1-\varepsilon(x)) \times \int_\Gamma W(x,y)q_0(y)\,d\Gamma_y u(x)\,d\Gamma_x. \tag{5.1}$$

We consider a Galerkin–Bubnov formulation and choose bilinear trial and basis functions $\phi_{k_{(k=l,\ldots,N)}}$ with local support $\Gamma_k \subset \Gamma$. Then the Galerkin equations read: find $q_{0,h}(x) = \sum_{i=1}^{N} q_0^{(i)} \phi_i(x) \in U_h$ such that

$$\sum_{i=1}^{N} q_0^{(i)} \underbrace{\int_{\Gamma j} \phi_i(x)\phi_j(x)\,\mathrm{d}\Gamma_x}_{=:M_{ij}} - \sum_{i=1}^{N} q_0^{(i)} \underbrace{\int_{\Gamma j} (1-\varepsilon(x)) \int_{\Gamma i} W(x,y)\phi_j(x)\phi_i(y)\,\mathrm{d}\Gamma_y\,\mathrm{d}\Gamma_x}_{=:S_{ij}} = \underbrace{\sigma \int_{\Gamma j} \varepsilon(x) T^4(x)\phi_j(x)\,\mathrm{d}\Gamma_x}_{=:f_j} \tag{5.2}$$

holds for all $j = 1, \ldots, N$. We can write (5.2) in the following short form:

$$Cq_0 := (M - S)q_0 = f \tag{5.3}$$

using the abbreviations $M := (M_{ij})_{i,j=1,\ldots,N}$ for the mass matrix, $S := (S_{ij})_{i,j=1,\ldots,N}$ for the view factor matrix and $f = (f_j)_{j=1,\ldots,N}$ for the right-hand side of the discretized equation.

The mass matrix M and the right-hand side f can be either calculated analytically exact for special geometries or numerical integration is applied. To keep the numerical integration error small, we handle the weak singularity of the integral kernel in the case of a non-smooth boundary by employing double partial integration, see [17,18].

5.2. Realization of the visibility function $V(x, y)$

The main problem is the efficient detection of the shadow zones to calculate the visibility function $V(x, y)$ appearing as part of the visibility matrix S for non-convex enclosures. To reduce the computational effort, in [11] a geometrical algorithm was developed to determine the shadow function in the two-dimensional case for polygonal domains. This algorithm was transformed to the 3D-case for an enclosure with polyhedral boundary and consists of the following steps: First we decide whether the geometry is convex or non-convex using an angle criterium. Then an element-orientated pre-view factor matrix is calculated to reduce the number of elements we have to deal with in the last step, the nodewise calculation of the view factors. With this algorithm we obtain reasonable results since less than 5% of all view factors have to be calculated numerically. For more details see [9,10,18].

Table 1
Solution methods for the unit square

n_l	Picard		Two-grid		Multi-grid		Cg-Method	
	Iter. steps	CPU time	Iter. steps	CPU time	Iter. steps	CPU time	Iter steps	CPU time
32	12	<1	4	<1	2	<1	14	<1
64	12	<1	4	<1	2	<1	15	<1
128	12	0.87	4	<1	2	<1	17	<1
256	12	3.45	4	1.5	2	<1	17	<1
512	12	13.6	4	6.07	2	2.03	17	<1
1024	12	53.7	4	24.5	2	8.9	17	4.05

6. Numerical test cases

6.1. Two-dimensional problems

Here we present a two-dimensional convex and non-convex geometries in order to compare the solution methods for the discrete equation (5.3), namely: the Picard iteration, the two-grid and multi-grid iterations and the conjugate gradient iteration. For more details on these iteration methods and their convergence analysis properties see [7,8,12,13,16]. As a convex enclosure we take a unit square for example and discretize its surface Γ into n elements. The emissivity coefficient is chosen as $\varepsilon = 0.5$, the Stefan–Boltzmann constant has the value $\sigma = 5.67 \times 10^{-8} \frac{\mathrm{W}}{\mathrm{m}^2\,\mathrm{K}^4}$ and the surface temperature is given by the function $T(t) = \frac{1}{2}(T_1 + T_2) - \frac{1}{2}(T_2 - T_1)\sin 2\pi t$ with $T_1 = 1000$ K and $T_2 = 2000$ K. Table 1 shows the numerical results for this case. It contains both the number of iteration steps and the CPU-time in seconds required by each iteration. The number n_l denotes the dimension parameter of the solved problem and l is the level number.

For a non-convex enclosure geometry we consider the curve shown in Fig. 5. In this case the visibility function $V(x, y)$ must be taken into account. Using the same values for ε, σ and T we obtain Table 2 which shows the numerical results for the non-convex problem.

6.2. Three-dimensional problem

As three-dimensional non-convex geometry we take an aperture as depicted below and use a quadrangular discretization of the surface Γ into 480 elements. The emissivity coefficient is chosen as $\varepsilon = 0.2$ and the temperature source is $T = 500\sqrt[4]{x(1.5 - x)y(0.5 - y)}$ K. The error is controlled a posteriori by the residual. Then the outgoing radiatve flux q_0 looks as follows:

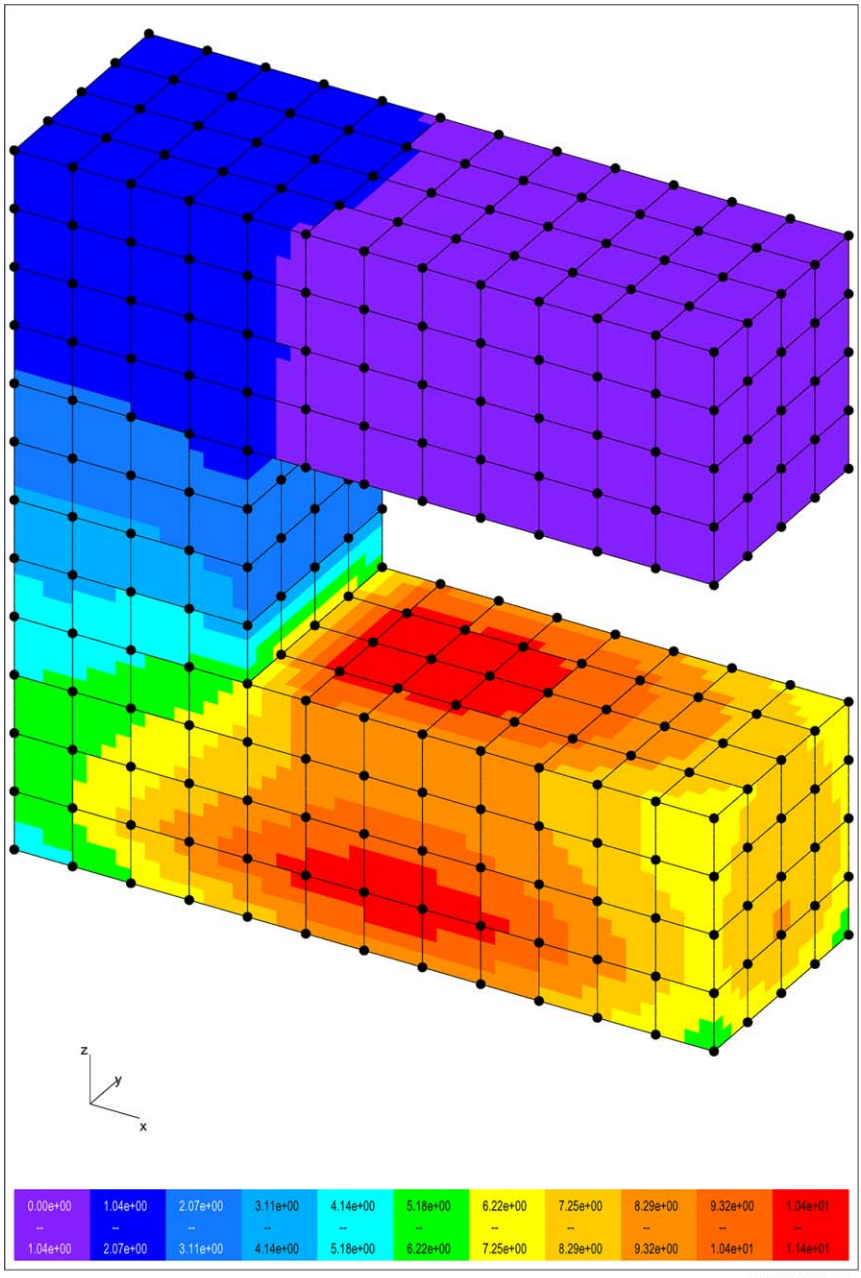
z
y
x
0.00e+00
--
1.04e+00
1.04e+00
--
2.07e+00
2.07e+00
--
3.11e+00
3.11e+00
--
4.14e+00
4.14e+00
--
5.18e+00
5.18e+00
--
6.22e+00
6.22e+00
--
7.25e+00
7.25e+00
--
8.29e+00
8.29e+00
--
9.32e+00
9.32e+00
--
1.04e+01
1.04e+01
--
1.14e+01
RMQXLib v3.0 (c) R. Quatember

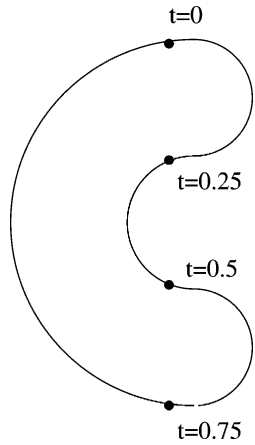

Fig. 5. Non-convex enclosure geometry.

Table 2
Solution methods for the non-convex curve in Fig. 5

n_l	Picard		Two-grid		Multi-grid		Cg-Method	
	Iter. steps	CPU time	Iter. steps	CPU time	Iter. steps	CPU time	Iter. steps	CPU time
32	14	<1	6	<1	4	<1	18	<1
64	14	<1	6	<1	4	<1	20	<1
128	14	1.4	6	<1	4	<1	23	<1
256	14	5.45	6	2.03	4	1.5	30	<1
512	14	21.2	6	8.4	4	5.8	30	1.8
1024	14	83.8	6	32.8	4	22.3	30	7.3

7. Conclusions

Throughout the formulation of the problem and due to the presence of the visibility function $V(x,y)$ which appears as a result of the heat radiation inside a non-convex enclosure geometries, one sees clearly the influence of this function on the analysis related to the properties of the integral operator. Moreover, its presence exhibits an extra important feature to the numerical simulation of the radiosity integral equation. The main problem was the efficient detection of the shadow zones to calculate the visibility function appearing as a part of the visibility matrix S for the non-convex geometries. To achieve a good numerical results a geometrical algorithm was developed to determine the shadow function in the two-dimensional case for polygonal domains and consequently this algorithm was transformed to the three-

dimensional case for an enclosure with polyhedral boundary. The efficiency of this algorithm has enabled us to obtain quite reasonable results since less than 5% of all view factors have to be calculated numerically. The numerical results for the two-dimensional convex and non-convex geometries shown in Tables 1 and 2 respectively illustrate clearly that both the two-grid and the multi-grid methods require less number of iteration steps in comparison to the other iterations. This demonstrates that one of the characteristic features of the multi-grid method is its fast convergence. The convergence speed does not deteriorate when the discretization is refined, where as other classical iterative methods slow down for decreasing grid size. As a consequence one obtains an acceptable approximation of the discrete problem at the expense of the computational work proportional to the number of unknowns, which is also the number of equations of the system. It is not only the complexity which is optimal, also the constant of proportionality is so small that other methods can hardly surpass the multi-grid efficiency. In regards to the numerical example on the three-dimensional non-convex geometry our experience shows that the conjugate gradient method with preconditioning has turned out to be the most efficient method for this case.

Acknowledgments

The first author of this paper would like to express his gratitude to Prof. Dr. Gerald Warnecke for the support and faithful cooperation during his stay at the Institute of Analysis and Numerics at Magdeburg University—Germany.

The second author would like to express her sincere thanks to Prof. Dr. W.L. Wendland who gave her the possibility and the support to work in the area of heat radiation as member of the Sonderforschungsbereich SFB 259 "Hochtemperaturprobleme rückkehrfähiger Raumtransportsysteme" at the University of Stuttgart.

References

[1] K.E. Atkinson, The Numerical Solution of Integral Equations of the Second Kind, Cambridge University Press, 1997.
[2] K.E. Atkinson, The planar radiosity equation and its numerical solution, IMA J. Numer. Anal. 20 (2000) 303–332.
[3] K.E. Atkinson, G. Chandler, The collocation method for solving the radiosity equation for unoccluded surfaces. Reports on Computational Mathematics, vol. 75, Department of Mathematics, University of Iowa, Iowa City, 1995.
[4] R. Bialecki, Boundary element calculation of the radiative heat sources, in: I.C. Wrobel, C.A. Brebbia, A.J. Nowak (Eds.), Advanced Comp. Meth. in Heat transfer II, vol. 1, Elsevier, London, 1992.

[5] R. Bialecki, Solving Heat Radiation Problems Using the Boundary Element Method, Comp. Mech. Publ., Southampton, 1993.
[6] D. Gaier, Integralgleichung erster Art und konforme Abbildungen, Math. Zeitschr. 147 (1976) 113–139.
[7] W. Hackbusch, Iterative Solution of Large Sparse Systems of Equations, Springer-Verlag, 1994.
[8] W. Hackbusch, Integral Equations. Theory and Numerical Treatment, Birkhäuser Verlag, 1995.
[9] O. Hansen, The radiosity equation on certain spaces of continuous functions and its numerical solution, Preprint No. 2, Johannes Gutenberg-Universität Mainz, 2001.
[10] O. Hansen, The local behavior of the solution of the radiosity equation on polyhedral domains in the $\mathbb{R}^3$, SIAM J. Math. Anal. 33 (3) (2001) 718–750.
[11] M. Maischak, Tätigkeitsbericht SFB 259, Teilprojekt B7, Mathematisches Institut A, Universitat Stuttgart, 1997.
[12] N. Qatanani, Lösungsverfahren und Analysis der Integralgleichung für das Hohlraum-Strahlungs-Problem. Doctoral thesis, Universität Stuttgart, (1996).
[13] N. Qatanani, Numerical treatment of the two-dimensional heat radiation integral equation, J. Comput. Anal. Appl., in press.
[14] N. Qatanani, M. Schulz, W.L. Wendland, The heat radiation problem: three-dimensional analysis and numerical solution methods for arbitrary enclosure geometries, in preparation.
[15] N. Qatanani, M. Schulz, Preconditioned conjugate gradient method for three-dimensional non-convex enclosure geometries with diffuse and grey surfaces, Appl. Math. Comput. 159 (2004) 797–807.
[16] N. Qatanani, Use of the multi-grid methods for heat radiation problems, J. Appl. Math. 6 (2003) 305–317.
[17] M. Schulz, H. Schulz, A new method for the computation of the view factor matrix for three dimensional heat radiation problems, in preparation.
[18] M. Schulz, W.L. Wendland, Mathematical analysis and numerical realization of heat radiation problems, in preparation.
[19] C. Schwab, W.L. Wendland, Kernel properties and representations of boundary integral operators, Math. Nachr. 156 (1992) 187–218.
[20] R. Siegel, J.R. Howell, Thermal Radiation Heat Transfer, third ed., Hemisphere Publishing Corp., New York, 1992.
[21] T. Tiihonen, Stefan–Boltzmann Radiation on Non-Convex Surfaces, Math. Meth. Appl. Sci. 20 (1997) 47–57.
[22] T. Tiihonen, A nonlocal problem arising from heat radiation on non-convex surfaces, Eur. J. Appl. Math. 8 (1998) 403–416.